Electronic Supplementary Material (ESI) for Journal of Materials Chemistry C.

A Combinational Molecular Design to Achieve Highly Efficient Deep Blue Electrofluorescence

Mengying Bian[a], Zifeng Zhao[b], Yu Li[a], Qing Li[c], Zhijian Chen[a,d,e], Dongdong Zhang[f], Shufeng Wang[a,*], Zuqiang Bian[b], Zhiwei Liu[b], Lian Duan[f,*], Lixin Xiao[a,d,e,*]

[a.] State Key Laboratory for Mesoscopic Physics and Department of Physics, Peking University, Beijing 100871, P. R. China E-mail: xiao66@pku.edu.cn
[b.] Beijing National Laboratory for Molecular Sciences, State Key Laboratory of Rare Earth Materials Chemistry and Applications, College of Chemistry and Molecular Engineering, Peking University, Beijing 100871, P. R. China E-mail: bianzq@pku.edu.cn
[c.] Valiant Corporation, Shandong 264006, P.R. China
[d.] Co-Innovation Center for Micro/Nano Optoelectronic Materials and Devices, Chongqing University of Arts and Sciences, Yongchuan Chongqing 402160, P.R. China
[e.] New Display Device and System Integration Collaborative Innovation Center of the West Coast of the Taiwan Strait，Fuzhou 350002, P.R. China
[f.] Key Lab of Organic Optoelectronics and Molecular Engineering of Ministry of Education, Department of Chemistry, Tsinghua University, Beijing 100084, P. R. China E-mail: duanl@mail.tsinghua.edu.cn

Supplementary photoluminescent properties

To further confirm that emission mechanism occurs in TPEA, the doped films in the polymethylmethacrylate (PMMA) host (5±1 *wt*.%) were fabricated and their transient PL decay and temperature dependence of the transient PL decay from 100 K to 300 K were shown as **Figure S1**. No long tail from delayed fluorescence was observed and no obvious variation of the emission with increasing temperature, which supports that TPEA is not a TADF material. The fluorescence lifetimes of the doped film at different wavelength are 1.9 ns, 2.1 ns, 2.3 ns and 2.6 ns at 420 nm, 440 nm, 460 nm and 480 nm, respectively, indicating that the fluorescence lifetime of the doped film depends on the measured wavelength, which indicates the existence of HLCT character in TPEA.

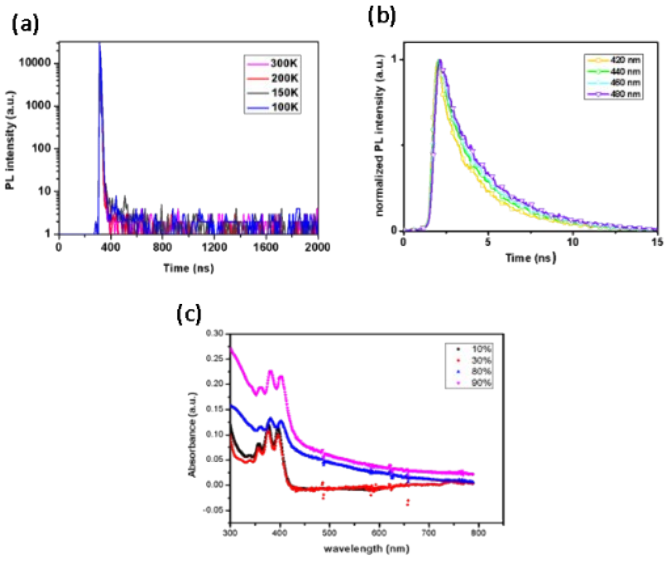

Figure S1. Temperature dependence of PL characteristics of a 5 *wt*.% TPEA:PMMA film: (a) PL decay curves of a 5 *wt*.% TPEA:PMMA film at 300 K (pink line), 200 K (red line), 150 K (olive line) and 100 K (blue line), the excitation wavelength of the films was 360 nm; (b) PL decay curves of a 5 *wt*.% TPEA:PMMA film at room temperature at the emission wavelength of 420 nm (yellow line), 440 nm (green line), 460 nm (blue line) and 480 nm (purple line). (c) Absoprtion spectra of TPEA in THF/H_2O mixtures with different water fractions (f_w).

Supplementary theoretical calculations

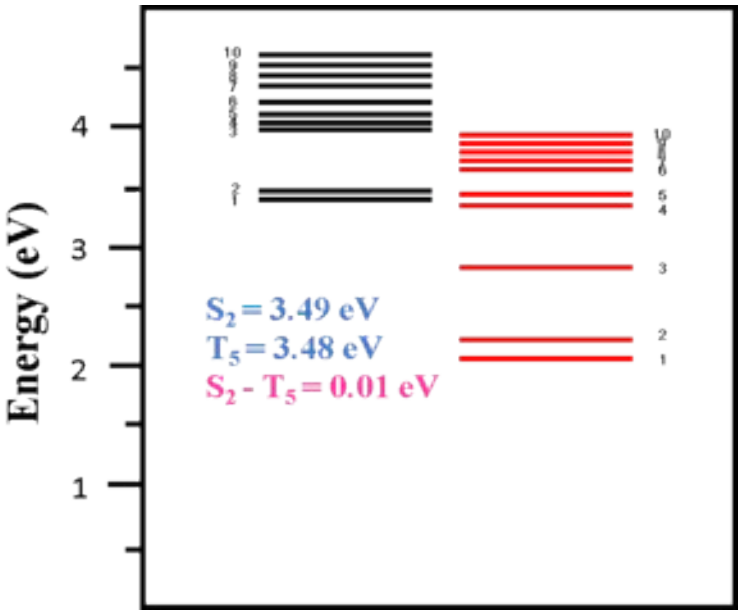

Figure S2. Energy diagram of the first ten singlet and triplet excited states of TPEA from TD-M06–2X calculations.

In order to further understand the nature of electronic transitions for different excited states, we employed the electron analysis function of Multiwfn software. The "particle" and "hole" contributions for the first ten singlet (S_0-S_n, n = 1-10) and triplet (S_0-T_n, n = 1-10) states of TPEA are presented in **Figure S3**. Pan *et al.* have reported the excited states of TADF material 4CzIPN and found that all "particles" and "holes" are localized on the carbazole groups and the dicyanobenzene core, respectively, demonstrating the represented CT transition feature. While for TPEA, we first focus on the transition of S_0-S_2, where the hole is mainly distributed on the anthracene near the methoxy unit with a little on the anthracene close to the cyano group, which is contrary to the particle, showing an excellent balance between spatial separation and orbital overlap. The coexistence of separated orbitals and orbital overlap means the coexistence of CT and LE components, which is in good agreement with the definition of the HLCT state. Similarly, S_3, S_6, S_7, S_8, S_9, S_{10}, T_3, T_5 and T_7 are characterized by HLCT. Referred from the energy level diagram, the energy gap (ΔE_{ST}) between S_1 and T_1 is 1.3 eV, which might be ascribed to the transition of LE. The energy gap between HLCT state S_2 (3.49 eV) and T_5 (3.48 eV) is only 0.01 eV (shown in **Figure S2**), which can enhance the possibility of RISC. Furthermore, the big difference between S_1 and T_1 also provides the possibility for TTF for TPEA to enhance the exciton utilization rate. According to the calculation results of TPEA, the mechanism may be attributed to the combination of TTF and HLCT.

(a)

	Hole	Particle	Transition charater		Hole	Particle	Transition charater
S_1			LE	S_6			HLCT
S_2			HLCT	S_7			HLCT
S_3			LE	S_8			HLCT
S_4			LE	S_9			HLCT
S_5			HLCT	S_{10}			HLCT

(b)

	Hole	Particle	Transition charater		Hole	Particle	Transition charater
T_1			LE	T_6			LE
T_2			LE	T_7			HLCT
T_3			HLCT	T_8			LE
T_4			LE	T_9			LE
T_5			HLCT	T_{10}			LE

Figure S3. (a) Hole-electron distribution and transition character of the first ten singlet states for TPEA; (b) Hole-electron distribution and transition character of the first ten triplet stated for TPEA.

Table S1. Summary of small-molecule conventional fluorescent deep-blue OLEDs with $CIE_y < 0.1$ and $\eta_{PE,max} > 3$ lm W^{-1} over the past decade.

Materials	Mechanism	V_{on} (V)	$\eta_{P,max}$ (lm W^{-1})	λ_{EL} (nm)	CIE (x, y)	ref
TPEA	TTF-HLCT	3.3	7.3	443	0.15, 0.09	This work
PCzSP	TTF	3.3	7.2	444	0.15, 0.09	[1]
BD3	TTF	3.7	5.6	432	0.15, 0.06	[2]
3a	HLCT	3.1	4.9	-	0.15, 0.08	[3]
PPI-2TPA	HLCT	3	4.6	-	0.15, 0.06	[4]
BiPI-1	-	2.8	4.55	440	0.15, 0.08	[5]
26-BTPIPy	-	2.8	4.35	440	0.15, 0.09	[6]
PMSO	-	3.2	4.0	445	0.15, 0.08	[7]
TPINCz	HLCT	3.1	3.7	440	0.15, 0.06	[8]
TPA-PA	-	3.8	3.4	428	0.16, 0.07	[9]
DPT-TPI	-	2.9	3.2	432	0.16, 0.07	[10]

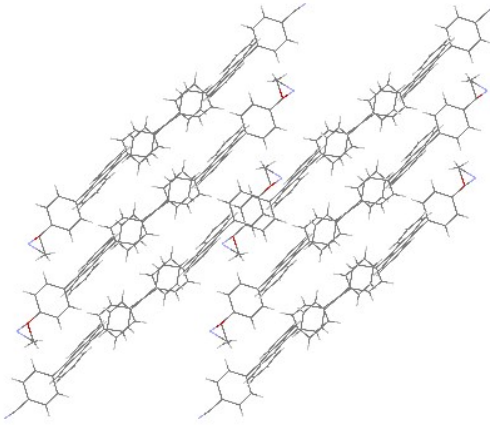

Figure S4. Oak Ridge Thermal Ellipsoid Plot view of the crystal structures of TPEA of the packing structure and the solvents were removed for clarity.

Table S2. Summary of the crystal data for TPEA

Parameter	TPEA
Empirical formula	$C_{69}H_{46}Cl_3NO$
Formula weight [g mol^{-1}]	1011.42
Temperature [K]	180
Wavelength [Å]	0.71073
Crystal system	Monoclinic
Space group	*C* 2/*c*
Crystal color and size [mm^{-3}]	Colorless, 0.326×0.246×0.049
a [Å]	13.1358 (8)
b [Å]	14.0526 (6)
c [Å]	28.8957 (13)
α [°]	90
β [°]	97.657 (6)
γ [°]	90
Volume [Å^3]	5286.4 (5)
Z	4
Density, calcd [g m^{-3}]	1.271
Absorption coefficient [mm^{-1}]	0.220
F(000)	2104
θ range for data collection [°]	3.60 to 26.02
Reflections collected	15922
Independent reflections	5175
R_{int}	0.0365
Restraints / parameters	30/362
Goodness-of-fit on F^2	1.042
Final R indices [I> 2σ(I)]	R_1 = 0.0558, wR_2 = 0.1276
R indices (all data)	R_1 = 0.0882, wR_2 = 0.1474

DFT calculaton data of TPEA

Table S3. Atom coordinates and absolute energies for **TPEA**

Standard orientation:

Center Number	Atomic Number	Atomic Type	Coordinates (Angstroms) X	Y	Z
1	6	0	3.750931	6.646096	0.738118
2	6	0	2.950055	6.932965	-0.369311
3	6	0	1.797638	6.187552	-0.613917
4	6	0	1.432686	5.123380	0.229318
5	6	0	2.242963	4.854073	1.345828
6	6	0	3.388658	5.607283	1.597985
7	6	0	0.182529	4.344289	-0.024457
8	6	0	-1.031792	5.172780	-0.295189
9	6	0	0.151682	2.978550	-0.009577
10	6	0	-1.853102	4.915916	-1.406465
11	6	0	-2.964859	5.712925	-1.674923
12	6	0	-3.281189	6.784127	-0.836920
13	6	0	-2.468399	7.058737	0.264874
14	6	0	-1.349523	6.269041	0.525668
15	6	0	-1.123189	2.199293	0.013841
16	6	0	1.391685	2.144543	-0.014904
17	6	0	-1.321013	1.117955	-0.861845
18	6	0	-2.495262	0.369749	-0.827670
19	6	0	-3.508193	0.656620	0.100559
20	6	0	-3.303598	1.722669	0.989586
21	6	0	-2.135575	2.480496	0.945953
22	6	0	1.543069	1.075458	0.884806
23	6	0	2.684098	0.276754	0.868581
24	6	0	3.707701	0.500340	-0.065001
25	6	0	3.549070	1.552872	-0.978962
26	6	0	2.414321	2.360223	-0.953281
27	6	0	-4.762262	-0.158377	0.146523
28	6	0	4.928617	-0.364396	-0.092078
29	6	0	-4.744397	-1.448540	0.722438
30	6	0	-5.953970	-2.241697	0.757687
31	6	0	-7.153828	-1.727201	0.218442
32	6	0	-7.172417	-0.434187	-0.350197

33	6	0	-5.963126	0.359628	-0.388197
34	6	0	-8.366571	0.121119	-0.915244
35	6	0	-8.378623	1.369831	-1.476801
36	6	0	-7.189002	2.148064	-1.518400
37	6	0	-6.022640	1.656770	-0.995385
38	6	0	-3.554977	-2.001767	1.299958
39	6	0	-3.546543	-3.249645	1.863690
40	6	0	-4.734367	-4.031174	1.893738
41	6	0	-5.896449	-3.540349	1.361293
42	6	0	6.145213	0.114498	0.443633
43	6	0	7.326311	-0.720691	0.415732
44	6	0	7.258354	-2.014432	-0.145386
45	6	0	6.044225	-2.495986	-0.681075
46	6	0	4.864746	-1.658726	-0.655347
47	6	0	5.940460	-3.797288	-1.272468
48	6	0	4.761021	-4.249974	-1.800624
49	6	0	3.602506	-3.425566	-1.779947
50	6	0	3.656464	-2.173255	-1.228859
51	6	0	6.247816	1.413664	1.040083
52	6	0	7.428575	1.868164	1.563896
53	6	0	8.590124	1.048361	1.533126
54	6	0	8.537419	-0.203422	0.980800
55	6	0	-8.402356	-2.553655	0.243542
56	6	0	8.479083	-2.880710	-0.170728
57	6	0	-9.377970	-2.371271	1.239680
58	6	0	-10.536409	-3.137898	1.263187
59	6	0	-10.754391	-4.116974	0.282653
60	6	0	-9.796381	-4.314062	-0.718010
61	6	0	-8.636305	-3.534149	-0.726571
62	6	0	8.677044	-3.869050	0.806745
63	6	0	9.808677	-4.678703	0.789583
64	6	0	10.773189	-4.511333	-0.217767
65	6	0	10.587102	-3.525870	-1.201259
66	6	0	9.450624	-2.723312	-1.172020
67	8	0	-11.921546	-4.817177	0.391632
68	6	0	11.941813	-5.342024	-0.241838
69	7	0	12.889929	-6.016068	-0.261396
70	6	0	-12.195093	-5.819086	-0.574490
71	1	0	4.644618	7.232674	0.933774

72	1	0	3.219923	7.742703	-1.042299
73	1	0	1.172097	6.425364	-1.469748
74	1	0	1.965034	4.050879	2.021293
75	1	0	3.995037	5.386760	2.472835
76	1	0	-1.611380	4.086468	-2.063843
77	1	0	-3.581259	5.500106	-2.544596
78	1	0	-4.148904	7.404466	-1.044891
79	1	0	-2.702802	7.892995	0.920983
80	1	0	-0.714378	6.496537	1.377233
81	1	0	-0.548076	0.868318	-1.583600
82	1	0	-2.631928	-0.451571	-1.526104
83	1	0	-4.067695	1.954429	1.726732
84	1	0	-2.000607	3.299174	1.645934
85	1	0	0.759748	0.875065	1.610558
86	1	0	2.785123	-0.533485	1.585840
87	1	0	4.321992	1.735112	-1.720878
88	1	0	2.314189	3.167056	-1.672554
89	1	0	-9.273101	-0.473218	-0.893335
90	1	0	-9.297992	1.767606	-1.898332
91	1	0	-7.206889	3.135364	-1.972402
92	1	0	-5.117914	2.253039	-1.037013
93	1	0	-2.648546	-1.407036	1.288948
94	1	0	-2.630915	-3.644080	2.296421
95	1	0	-4.718644	-5.018464	2.347770
96	1	0	-6.802508	-4.134897	1.394066
97	1	0	6.821637	-4.428776	-1.301464
98	1	0	4.709568	-5.240784	-2.243874
99	1	0	2.673614	-3.791071	-2.209191
100	1	0	2.772966	-1.545113	-1.223779
101	1	0	5.364033	2.040935	1.072732
102	1	0	7.479710	2.857545	2.010249
103	1	0	9.521125	1.416568	1.955625
104	1	0	9.425288	-0.825986	0.970007
105	1	0	-9.221287	-1.616809	2.006025
106	1	0	-11.288807	-2.998115	2.033293
107	1	0	-9.938465	-5.061583	-1.490189
108	1	0	-7.898667	-3.694662	-1.508476
109	1	0	7.933565	-4.000334	1.587488
110	1	0	9.953364	-5.438972	1.550549

111	1	0	11.331781	-3.397587	-1.980370
112	1	0	9.309081	-1.963267	-1.934819
113	1	0	-13.162601	-6.243481	-0.300042
114	1	0	-12.258292	-5.398293	-1.586886
115	1	0	-11.435157	-6.611782	-0.561569

Total Energy (RB3LYP) = -2748.33600139 Hartree

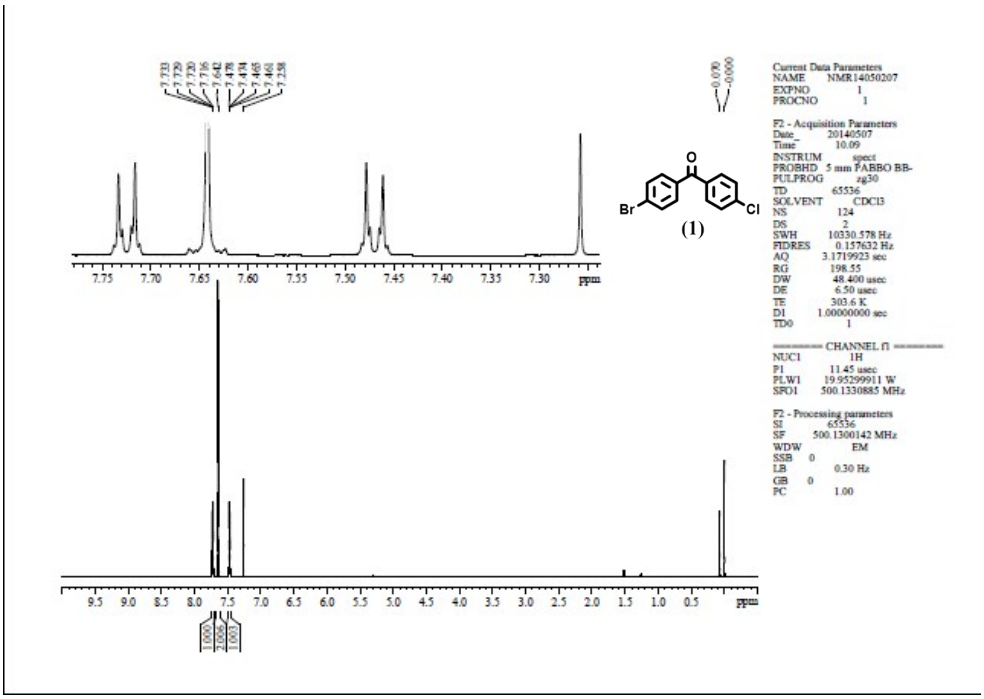

Figure S5. [1]H NMR of compound (1).

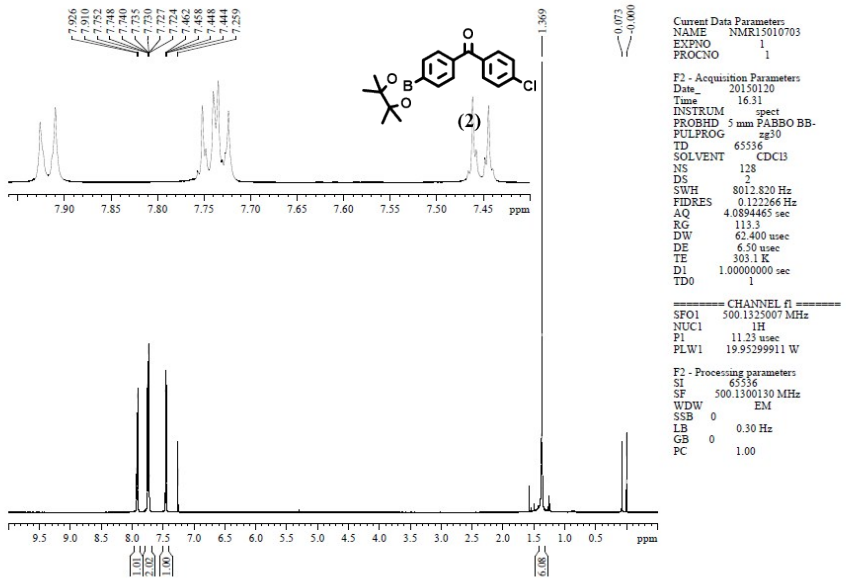

Figure S6. [1]H NMR of compound (2).

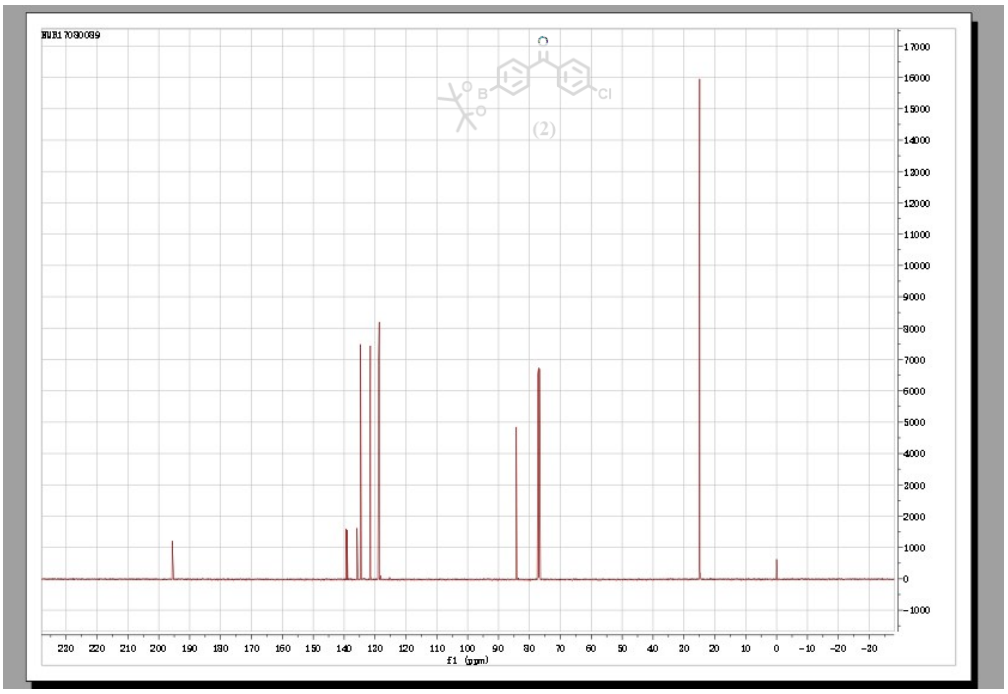

Figure S7. ^{13}C NMR of compound (2).

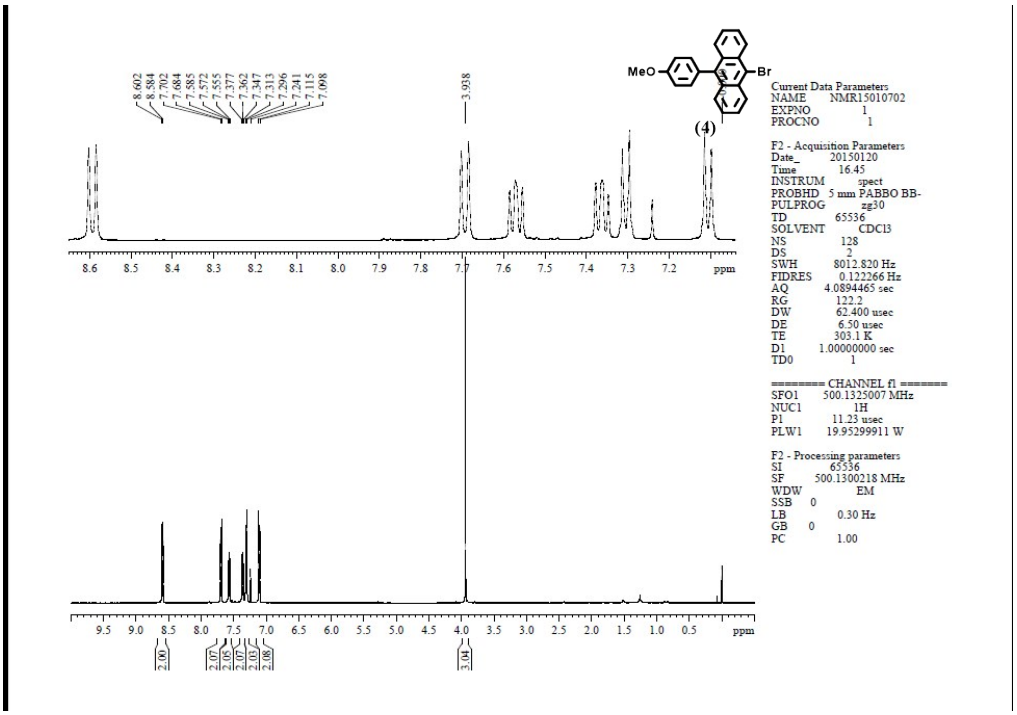

Figure S8. ^{1}H NMR of compound (4).

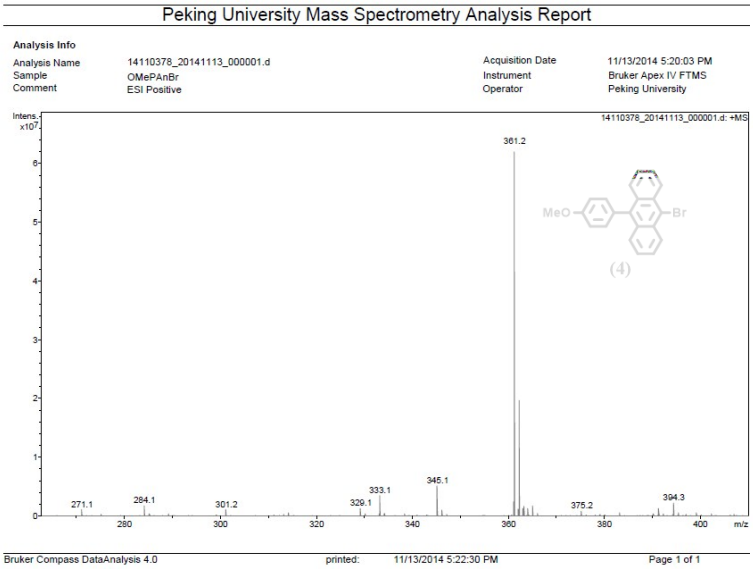

Figure S9. ESI-MS of compound (4).

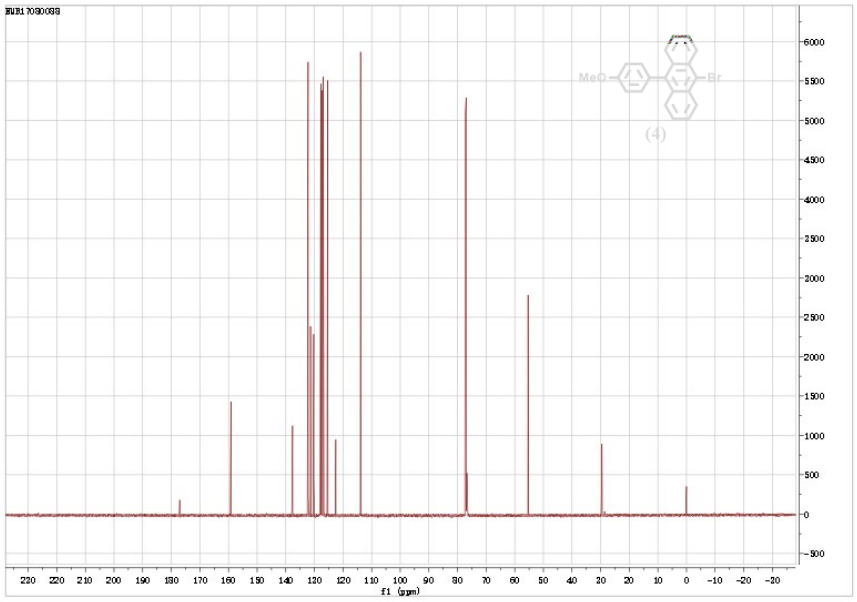

Figure S10. ^{13}C NMR of compound (4).

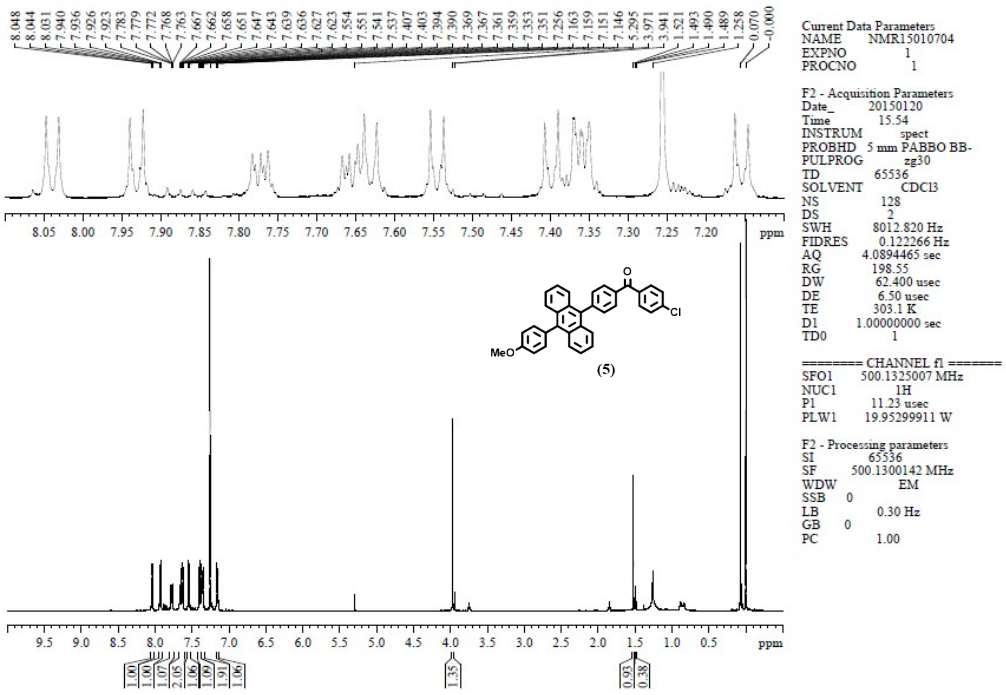

Figure S11. [1]H NMR of compound (5).

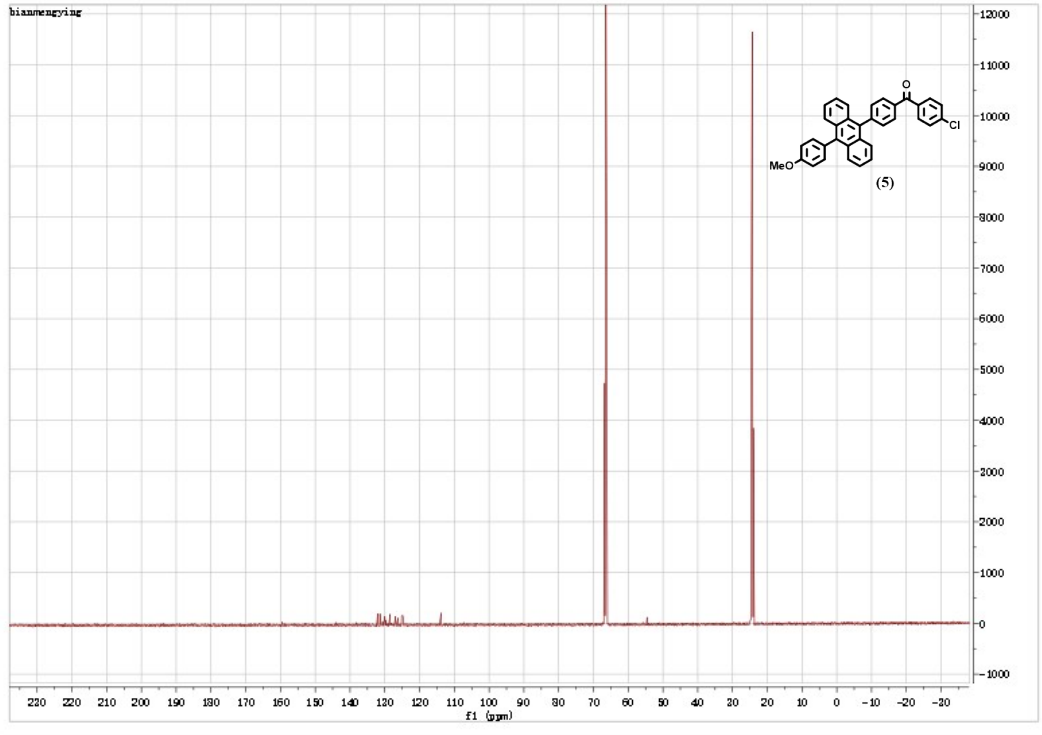

Figure S12. [13]C NMR of compound (5).

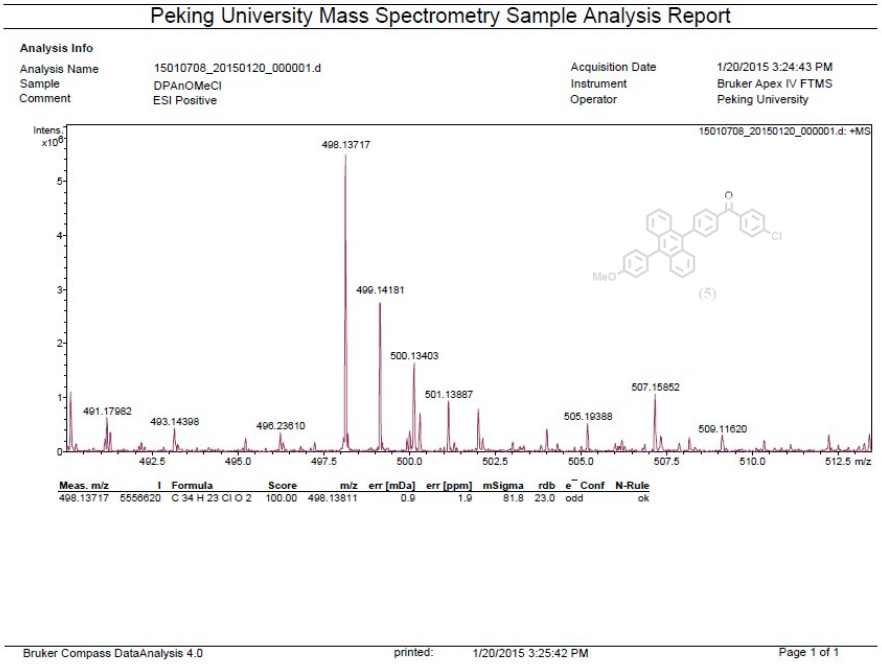

Figure S13. HRMS of compound (5).

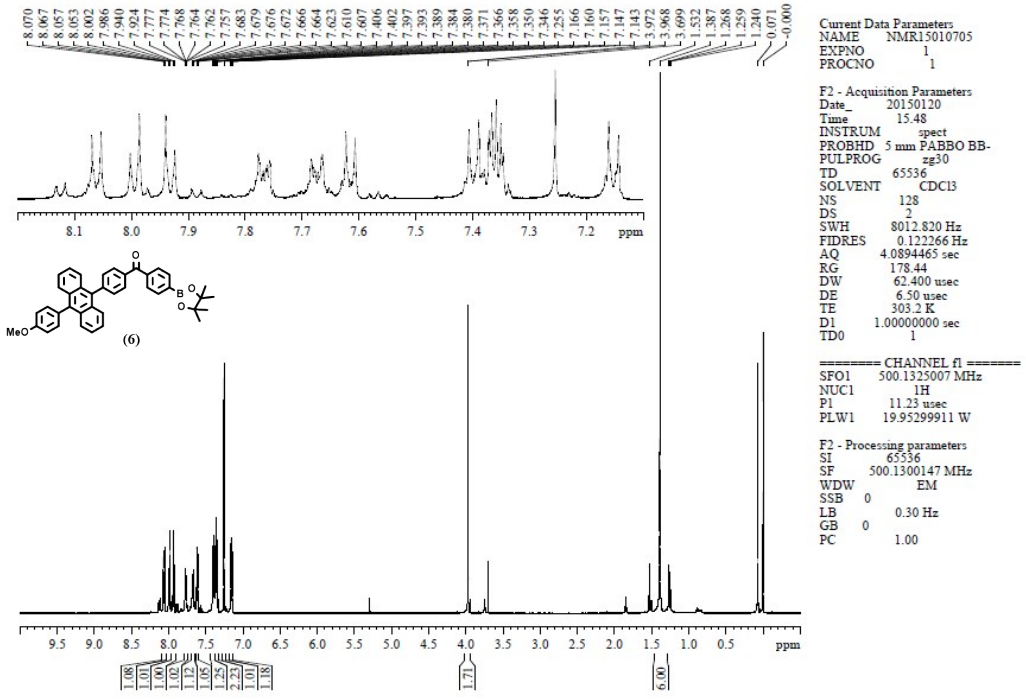

Figure S14. ^{1}H NMR of compound (6).

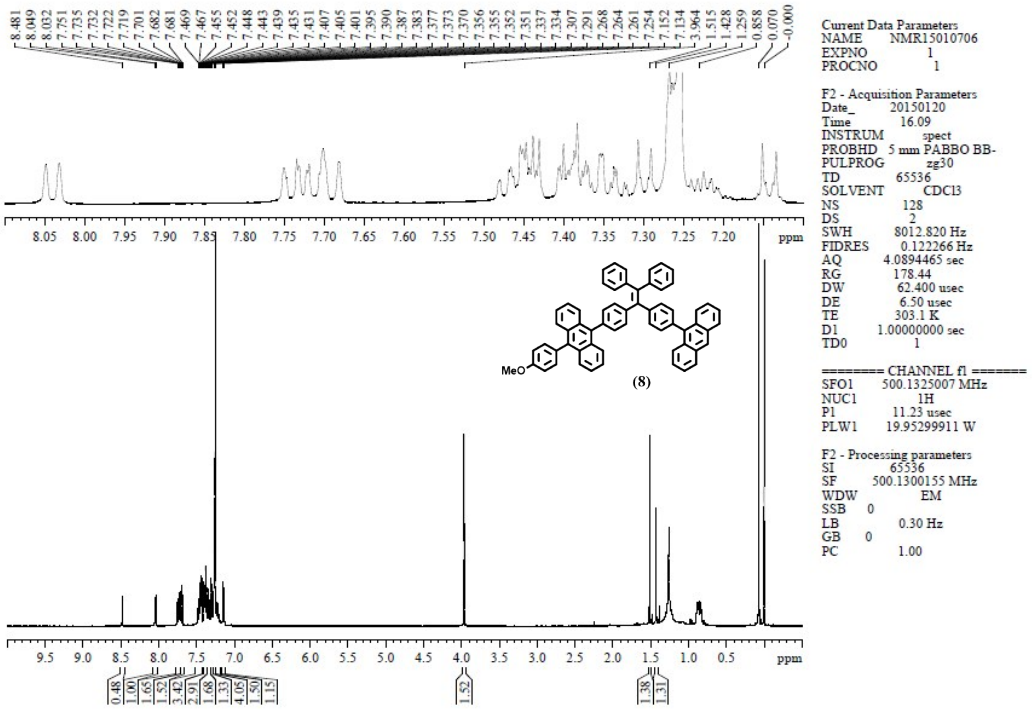

Figure S15. [1]H NMR of compound (8).

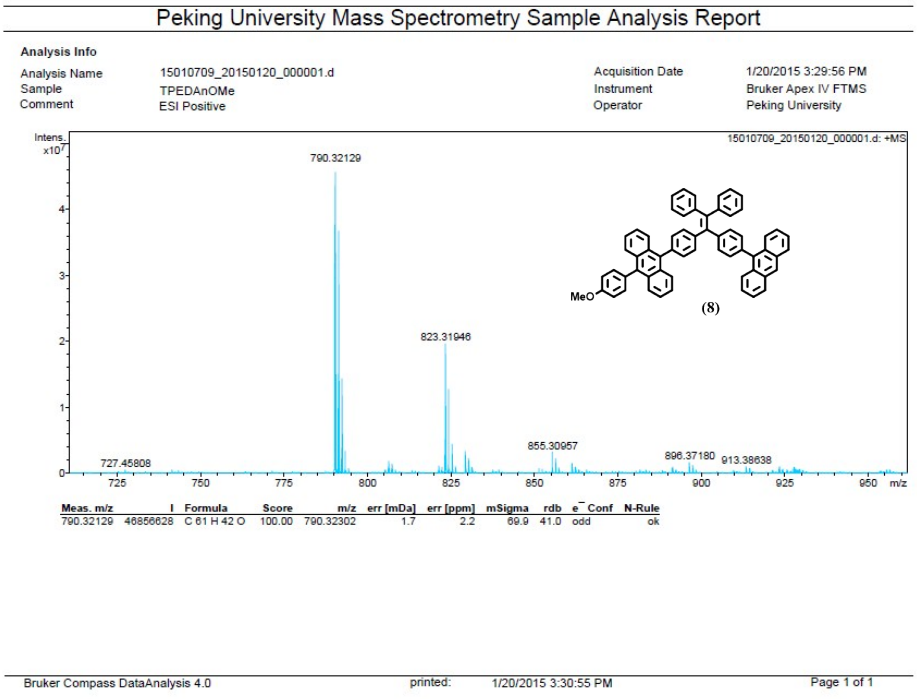

Figure S16. HRMS of compound (8).

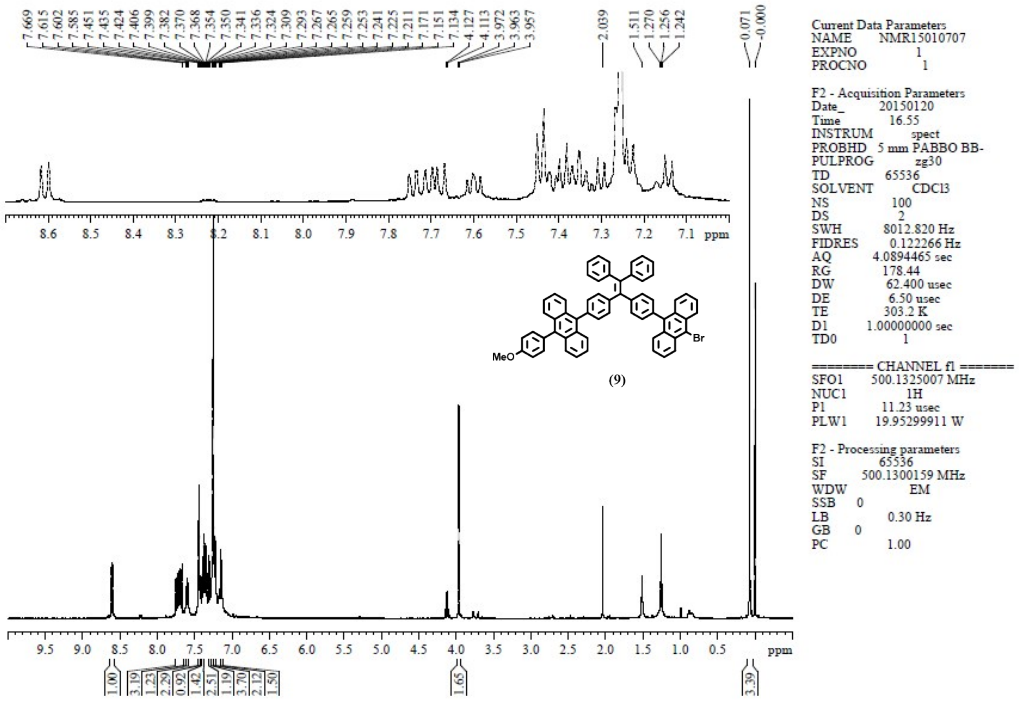

Figure S17. ^{1}H NMR of compound (9).

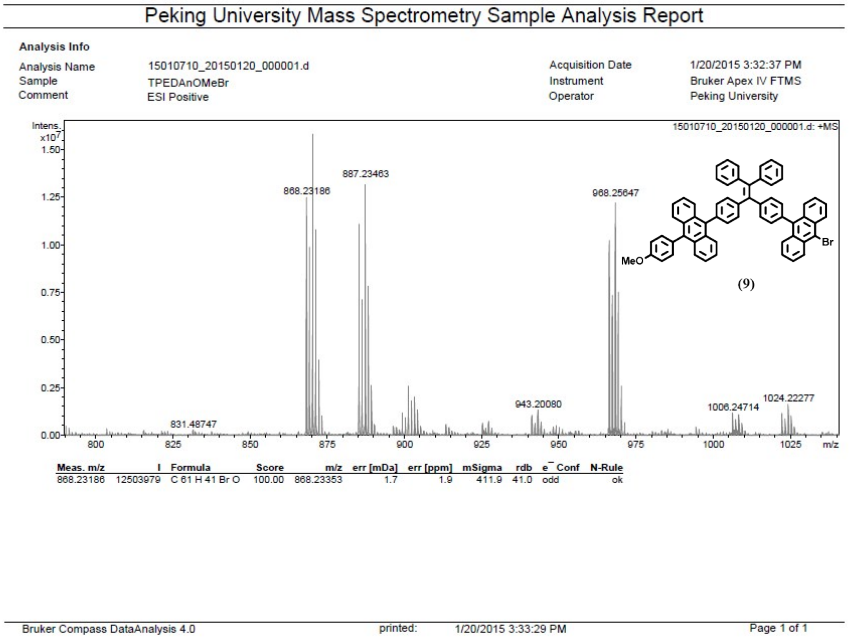

Figure S18. HRMS of compound (9).

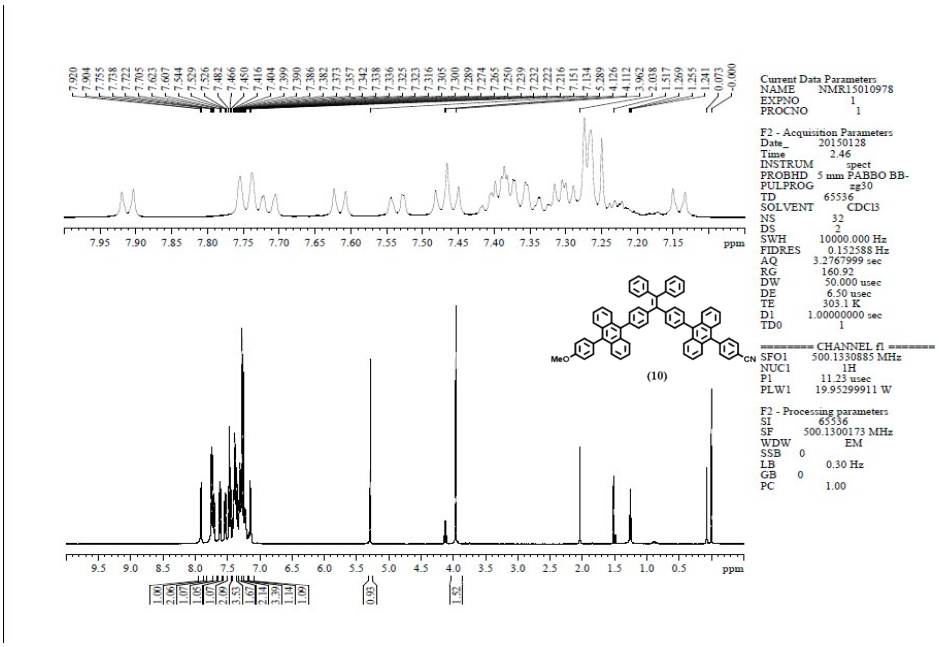

Figure S19. ^{1}H NMR of compound (10).

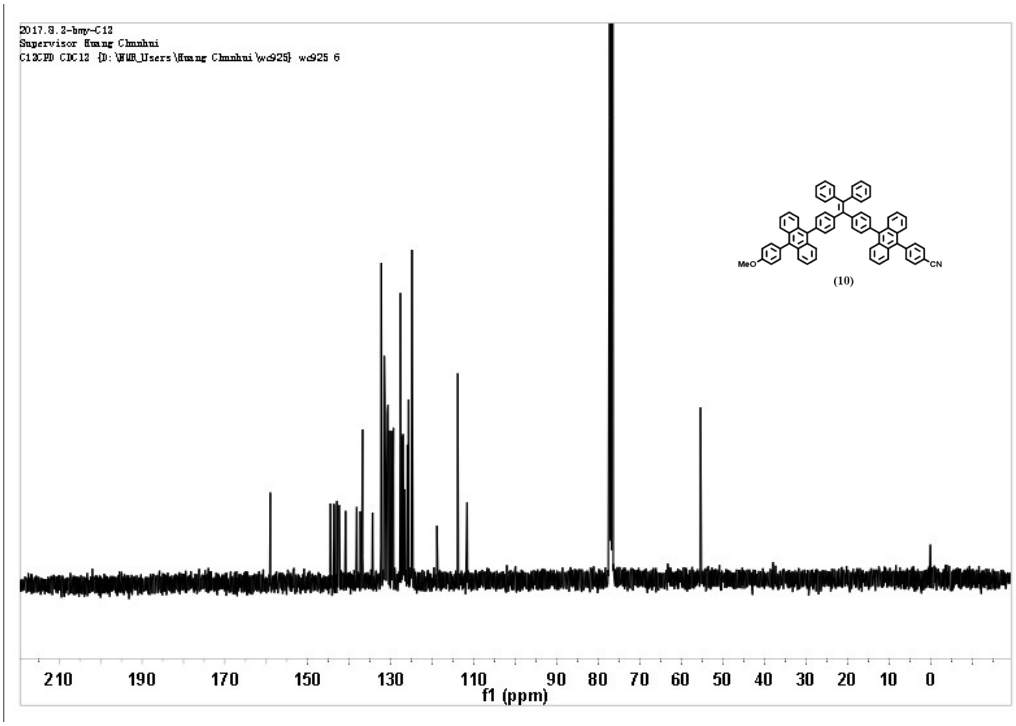

Figure 20. ^{13}C NMR of compound (10).

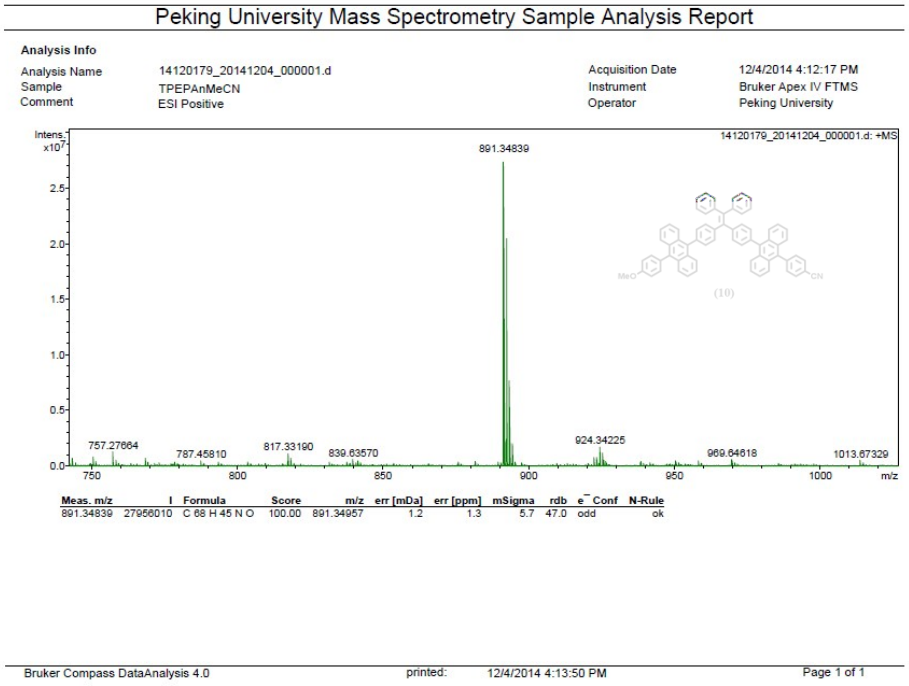

Figure S21. HRMS of compound (10).

Reference

1. Y.-H. Chen, C.-C. Lin, M.-J. Huang, K. Hung, Y.-C. Wu, W.-C. Lin, R.-W. Chen-Cheng, H.-W. Lin and C.-H. Cheng, *Chemical Science*, 2016, **7**, 4044-4051.
2. J.-Y. Hu, Y.-J. Pu, F. Satoh, S. Kawata, H. Katagiri, H. Sasabe and J. Kido, *Adv. Funct. Mater.*, 2014, **24**, 2064-2071.
3. B. Li, G. Tang, L. Zhou, D. Wu, J. Lan, L. Zhou, Z. Lu and J. You, *Adv. Funct. Mater.*, 2017, **27**, 1605245.
4. B. Liu, Z.-W. Yu, D. He, Z. Zhu, J. Zheng, Y.-D. Yu, W. Xie, Q.-X. Tong and C.-s. Lee, *Journal of Materials Chemistry C*, 2017, 5, 5402-5410.
5. Z.-L. Zhu, M. Chen, W.-C. Chen, S.-F. Ni, Y.-Y. Peng, C. Zhang, Q.-X. Tong, F. Lu and C.-S. Lee, *Org. Electron.*, 2016, **38**, 323-329.
6. Z.-L. Zhu, W.-C. Chen, L.-D. Zhang, X.-L. Liu, Q.-X. Tong, F.-L. Wong, F. Lu and C.-S. Lee, *Journal of Materials Chemistry C*, 2016, **4**, 6249-6255.
7. X. Tang, Q. Bai, Q. Peng, Y. Gao, J. Li, Y. Liu, L. Yao, P. Lu, B. Yang and Y. Ma, *Chem. Mater.*, 2015, **27**, 7050-7057.
8. W.-C. Chen, Y. Yuan, S.-F. Ni, Q.-X. Tong, F.-L. Wong and C.-S. Lee, *Chemical Science*, 2017, **8**, 3599-3608.
9. S. Tang, W. Li, F. Shen, D. Liu, B. Yang and Y. Ma, *J. Mater. Chem.*, 2012, **22**, 4401-4408.
10. Y. Yuan, J.-X. Chen, F. Lu, Q.-X. Tong, Q.-D. Yang, H.-W. Mo, T.-W. Ng, F.-L. Wong, Z.-Q. Guo, J. Ye, Z. Chen, X.-H. Zhang and C.-S. Lee, *Chem. Mater.*, 2013, **25**, 4957-4965.